Electrical analysis of light-weight, triangular weave reflector antennas

Knud Pontoppidan

TICRA
Laederstraede 34
DK-1201 Copenhagen K
Denmark
Email: kp@ticra.com

INTRODUCTION

The new light-weight reflector antenna technology being developed by several spacecraft companies requires accurate electromagnetic modelling of the reflector surface properties. In particular, the new tri-axially woven fibre skins are of interest.

In a recent study for ESTEC a new computer program has been developed in a co-operation between TICRA and Politecnico di Torino. The name of the program is MESTIS[1], MEtallic STrIps Simulator, and by means of this it is possible to model one or more layers of strip grids and each layer can consist of up to three strip grids making arbitrary angles with each other. In this way it is possible in particular to model the new triangular weave materials.

MESTIS is developed entirely by Politecnico di Torino and TICRA's role in the co-operation has been to ensure that the output can be used for reflector antenna analysis software such as GRASP8. To this end an auxiliary program converts the scattering matrix parameters from MESTIS into the reflection and transmission coefficients required by GRASP8.

In the following sections the electrical properties of the triangular weave will be illustrated as a function of some simple geometrical parameters of the material. The performance for a reflector antenna with a typical, triangular weave surface is calculated and the consequences are identified.

MECHANICAL AND ELECTRICAL MODELLING OF THE TRIANGULAR WEAVE MATERIAL

The geometrical structure of the triangular weave is illustrated in Fig. 1. Three sets of parallel wire grids are tilted 120º with each other. One notices that one set of wires passes alternately above and below the wires of the other sets. The intersection between one set and the two others takes place in the middle between the intersections between these two other sets.

The material in Fig. 1 can easily be bent over a dual curved surface with only a minor deformation of the mesh pattern. Once the wires are glued together a very light weight but yet form stable reflector shell is obtained.

To arrive at the electrical model it is assumed that all the wires are lying in the same plane and that they are in electrical contact at all intersection points. With this assumption we obtain the model shown in Fig. 2 which we can consider as three co-planar strip grids each with the spacing s and the strip width w.

The reflection and transmission properties of the structure in Fig. 2 can be analysed by MESTIS. It is possible to take into account the finite conductivity of the strip grid material and also dielectric layers on both sides of the strip grid can be considered. In order to make the present investigation simple it is assumed in the following that the strip material is a perfect conductor and no dielectrics are present. The structure in Fig. 2 can therefore be completely described by the two parameters, s/λ and w/λ, where λ is the wavelength.

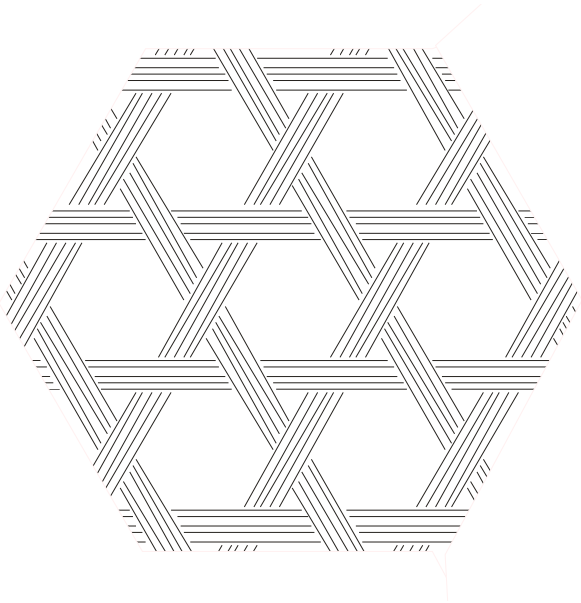

Fig. 1. The triangular mesh showing the interleaved sets of carbon fibres

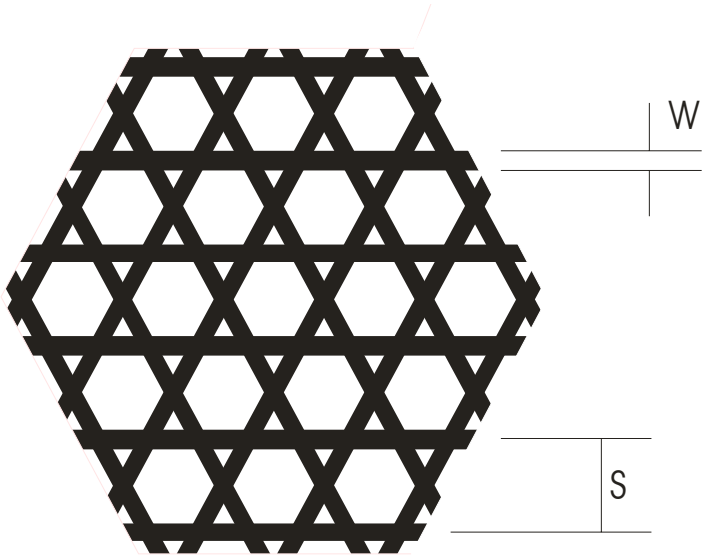

Fig. 2 The electrical model of the triangular weave.

REFLECTION PROPERTIES OF THE TRIANGULAR WEAVE

A planar sample of a general reflector material is illustrated in Fig. 3. The direction of an incident plane wave is given by the spherical coordinates (θ_i, ϕ_i), where θ_i is measured from the positive z-axis and ϕ_i from the positive x-axis. The angle θ_i is limited to the range $0° \le \theta_i < 90^o$.

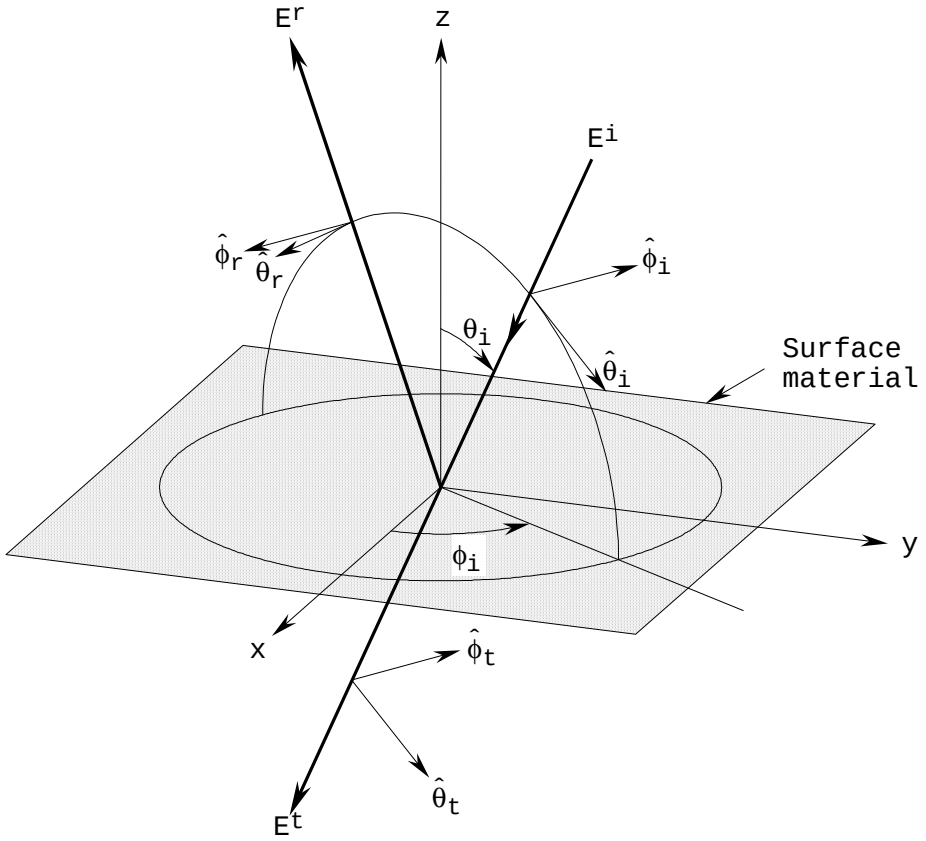

Fig. 3 Unit vectors for the definition of reflection and transmission coefficients in GRASP8.

The incident plane wave can be decomposed as

$$\overline{E}^i = E_\theta^i \hat{\theta}_i + E_\phi^i \hat{\phi}_i \tag{1}$$

and is partly reflected and partly transmitted through the surface where the unit vectors of incidence, $\hat{\theta}_i$ and $\hat{\phi}_i$ are the usual polar vectors shown in Fig. 3.

The reflected field is given by

$$\overline{E}^r = E_\theta^r \hat{\theta}_r + E_\phi^r \hat{\phi}_r \quad , \tag{2}$$

where

$$\begin{Bmatrix} E_\theta^r \\ E_\phi^r \end{Bmatrix} = \begin{Bmatrix} R_{\theta\theta} & R_{\phi\theta} \\ R_{\theta\phi} & R_{\phi\phi} \end{Bmatrix} \begin{Bmatrix} E_\theta^i \\ E_\phi^i \end{Bmatrix} \tag{3}$$

and the unit vectors of reflection, $\hat{\theta}_r$ and $\hat{\phi}_r$ are the negative mirror images of $\hat{\theta}_i$ and $\hat{\phi}_i$, respectively. This definition implies for example that the reflection coefficients for a perfect conductor are $R_{\theta\theta} = R_{\phi\phi} = +1$ and $R_{\phi\theta} = R_{\theta\phi} = 0$. Similar relations can be set up for the transmitted field.

The coefficients $R_{\theta\theta}$ and $R_{\phi\phi}$ represent the coupling from the incident to the reflected θ- and ϕ-components, respectively. These components are also referred to as R_{TMTM} and R_{TETE}, respectively.

Typical values for the triangular grid in Fig. 2 can be $s/\lambda = 1/20$ and $w/s = 1/10$. The MESTIS software has been used to calculate the four reflection coefficients for these values and for the incidence angles $0° \le \theta_i \le 60°$ and $0° \le \phi \le 360°$. The results for $R_{\theta\theta}$ and $R_{\phi\phi}$ are presented by the plots in Fig. 4. The results for the off-diagonal elements are not shown because they are very small, more than 80 dB down.

Two important characteristics are readily identified from Fig. 4. The triangular grid in Fig. 2 is very regular with symmetry planes every 30º in ϕ. This will limit the possible variation in ϕ and the results in Fig. 4 show that in practice the reflection coefficients are constant in ϕ. This is a very useful conclusion since it means that it is only necessary to investigate the variation with θ.

The other observation from Fig. 4 is that $R_{\theta\theta}$ decreases with increasing θ whereas $R_{\phi\phi}$ increases. This can have an effect in circular polarisation for offset reflector antennas, as will be demonstrated in the next section.

At normal incidence, $\theta = 0°$, $R_{\theta\theta} = R_{\phi\phi} = -0.06$ dB. This is due to a small amount of transmission through the grid. When the triangular weave is used for a reflector antenna the peak gain will be reduced by the same amount.

If the grid spacing, s/λ, is increased the mesh becomes more open and the reflection coefficients will decrease. This is illustrated in Fig. 5 which shows $R_{\theta\theta}$ and $R_{\phi\phi}$ as functions of θ for different values of s/λ. In this graph the strip width relative to the spacing is kept constant, $w/s = 0.1$. Fig. 5 shows for example that if the strip spacing is increased to $s/\lambda = 0.2$ the transmission loss increases to about 0.9 dB.

The variation with the strip width is shown in Fig. 6 for the constant value of the strip spacing, $s/\lambda = 1/20$.

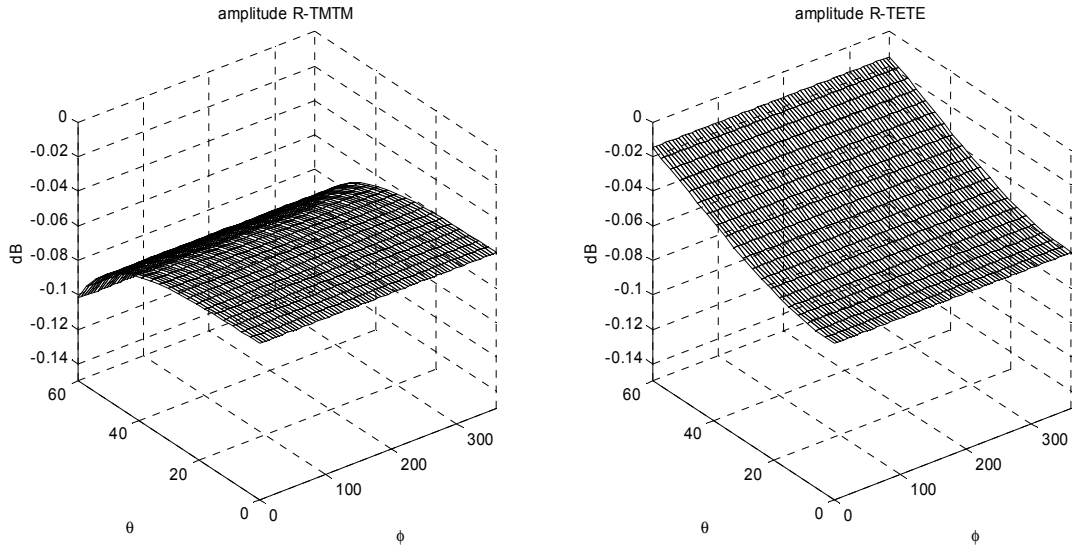

Fig. 4 The reflection coefficients $R_{\theta\theta}$ (left) and $R_{\phi\phi}$ (right) versus the angle of incidence (θ, ϕ)

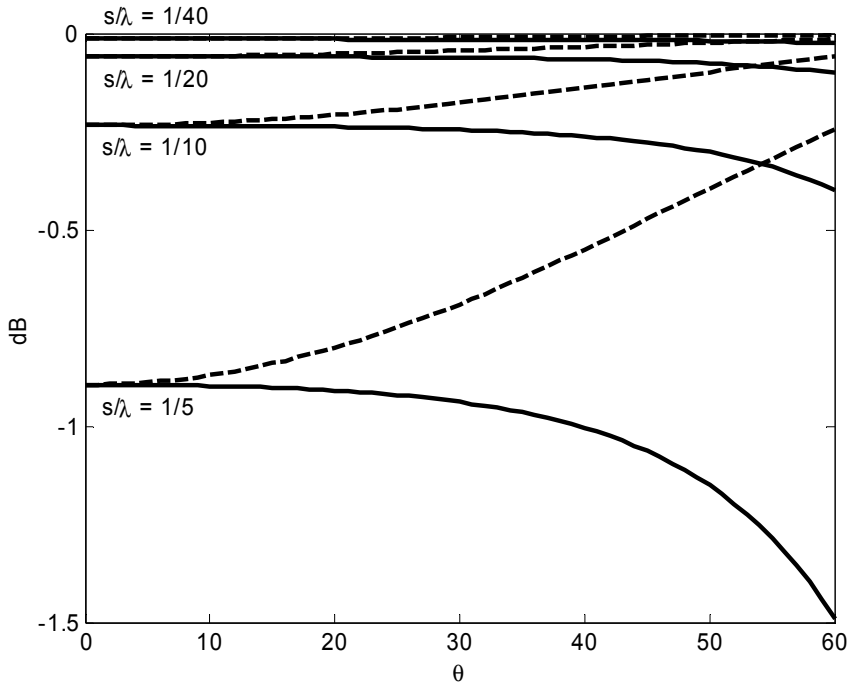

Fig. 5 The reflection coefficients $R_{\theta\theta}$ (full line) and $R_{\phi\phi}$ (dotted line) versus the angle of incidence from the normal θ with the strip spacing relative to the wavelength, s/λ, as parameter. The strip width relative to the strip spacing is constant 0.1.

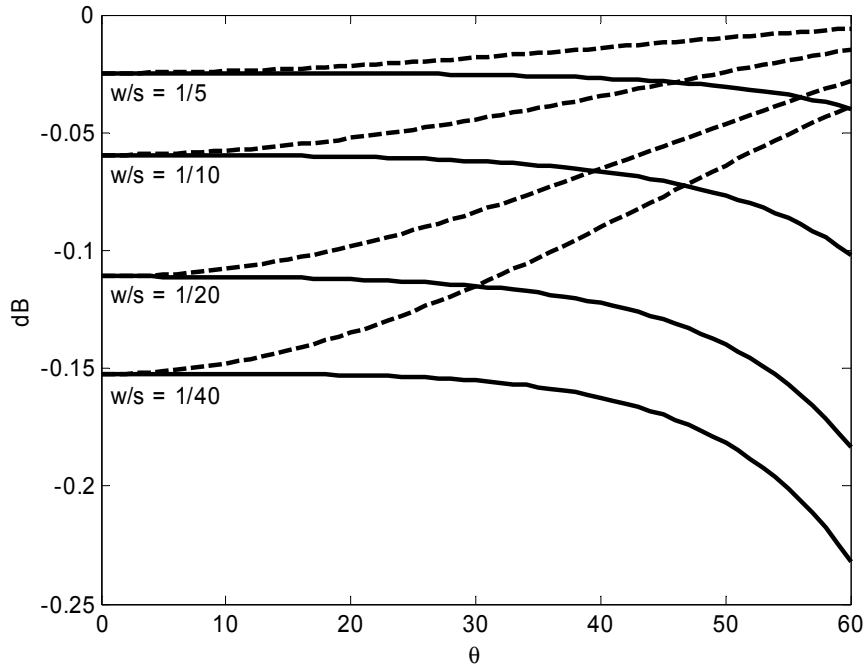

Fig. 6 The reflection coefficients $R_{\theta\theta}$ (full line) and $R_{\phi\phi}$ (dotted line) versus the angle of incidence from the normal θ with the strip width relative to the spacing, w/s, as parameter. The strip spacing relative to the wavelength is constant 1/20.

APPLICATIONAL EXAMPLE

In this section we will illustrate the influence of the triangular weave material for a single offset reflector antenna. The diameter is $D = 50\lambda$ and the focal length is $f = D$. The feed is located at the focus and it is a simple Gaussian beam operating in circular polarisation. The antenna is illustrated in Fig. 7.

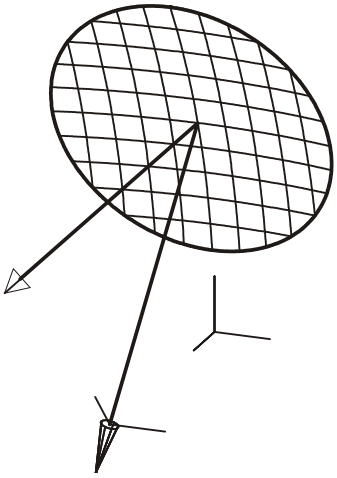

Fig. 7 Offset reflector antenna

Fig. 8 shows the radiation pattern in the plane of asymmetry both for a solid reflector and for a reflector constructed as a triangular weave with the typical parameters, $s/\lambda = 1/20$ and $w/s = 1/10$. For the solid reflector the co-polar component exhibits the typical beam squint in circular polarisation and the cross-polar lobes are very low, about 60 dB below the co-polar beam peak.

For the triangular weave the co-polar component in Fig. 8 is indistinguishable from the solid reflector (although there is a transmission loss of 0.06 dB). However, the difference between $R_{\theta\theta}$ and $R_{\phi\phi}$ generates a cross-polar component with the same shape as the co-polar beam and the maximum cross-polar lobe is now only about 45 dB below the co-polar peak. This result shows that with a slightly larger s/λ the cross-polar performance could soon become critical.

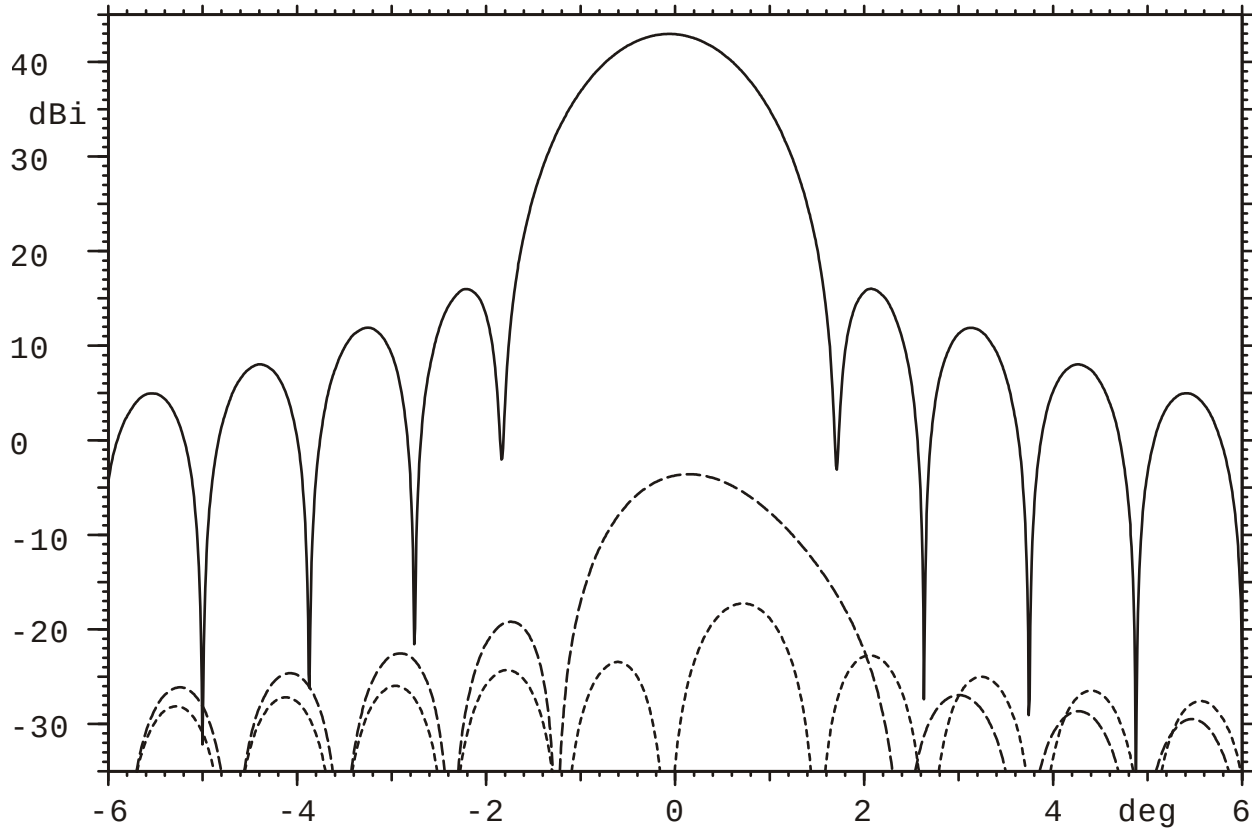

Fig. 8 The radiation pattern in the plane of asymmetry for the antenna in Fig. 7. The full line curve shows the co-polarisation for both the solid reflector and the triangular weave. The curves with short dots and long dots is the cross polarisation for the solid reflector and the triangular weave, respectively.

CONCLUSIONS

This paper has demonstrated how the reflection properties of a triangular weave can be determined by the MESTIS software developed by Politecnico di Torino. It is shown that the reflection coefficients are almost independent of the azimuthal variation of the angle of incidence but they do depend on the angle from normal incidence. It is demonstrated by an example how this can affect the cross polarisation performance for an offset reflector system operating in circular polarisation.

REFERENCES

[1] R. Orta, R. Tascone, and D.Trinchero, “USER MANUAL, Metallic Strip Simulator”, Dipartimento di Elettronica and IRITI-CNR, Politecnico di Torino, October 2001.